



# Synthesis and characterization of a novel and reusable $\text{Fe}_3\text{O}_4@$ THAM- $\text{CH}_2\text{CH}_2\text{-SCH}_2\text{CO}_2\text{H}$ magnetic nanocatalyst for highly efficient preparation of xanthenes and 3-aminoisoxazoles in green conditions

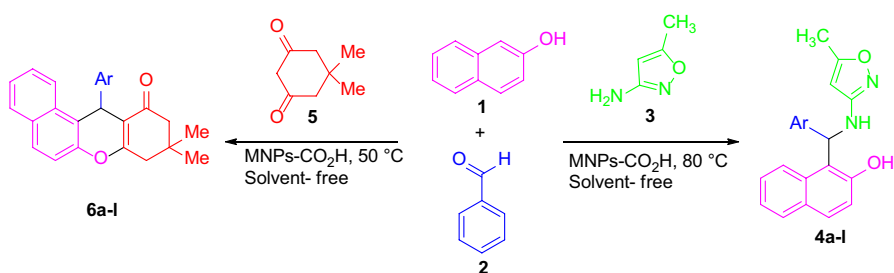
Mahboobeh Rezaie Kakhhaie<sup>1</sup> · Nourallah Hazeri<sup>1</sup> ·  
Malek Taher Maghsoodlou<sup>1</sup> · Afshin Yazdani-Elah-Abadi<sup>2</sup>

Received: 25 April 2021 / Accepted: 28 July 2021  
© The Author(s), under exclusive licence to Springer Nature B.V. 2021

## Abstract

In the present study, the synthesis and catalytic application of a novel thioglycolic acid doped on  $\text{Fe}_3\text{O}_4$  nanomagnetic particles coated with tris(hydroxymethyl)aminomethane (THAM) and 1,2-dichloroethane are described. The morphology, structure, and physicochemical properties have elucidated by several analytical methods like FT-IR, TEM, VSM, XRD, TGA, and FE-SEM. This nanocatalyst has successfully applied as a heterogeneous acid catalyst in the synthesis of diversely substituted biologically important xanthene and 3-aminoisoxazole derivatives. This catalyst eliminates our need for long-time reaction and hard catalyst separation from product, and it can be easily recovered with an external magnet for eight consecutive times without a significant decrease in its catalytic properties.

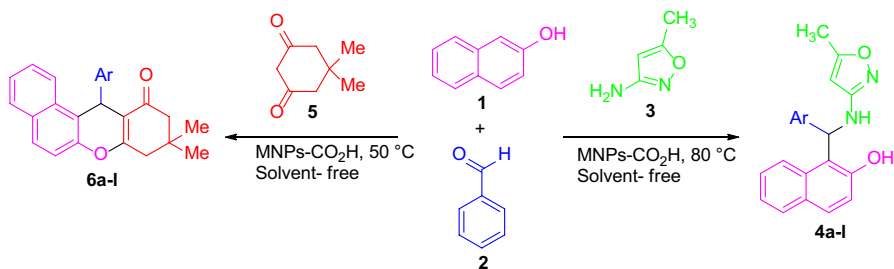
## Graphic abstract



**Keywords** Benzoxanthenes · Green chemistry · Magnetically recoverable nanocatalyst · MNP-CO<sub>2</sub>H · 3-Aminoisoxazole

✉ Nourallah Hazeri  
nhazeri@chem.usb.ac.ir; n\_hazeri@yahoo.com

Extended author information available on the last page of the article



**Scheme 1** One-pot, three-component synthesis of 3-aminoisoxazolmethylnaphthol and 12-aryl-8,9,10,12-tetrahydrobenzo[*a*]xanthen-11-one derivatives in the presence of MNPs-CO<sub>2</sub>H as catalyst

## Introduction

Recently, with regard to green chemistry, efficient, and economical chemical processes using nanocatalysts for the production of fine chemical and pharmaceutical products through multi-component reactions (MCRs) have become the subject of much interest in universities and industry [1–3]. Nanomaterial applications as heterogeneous catalysts have played a critical role at the interface of these fields. Nanocatalysts consist of an inner core material and an outer shell. Their properties can be changed by loading the acidic or alkaline groups on the core [4, 5]. The separation of nanocatalysts from the reaction medium limits their applications.

To solve this challenge, magnetic nanocatalysts (MNCs) have emerged as attractive candidates, which can be separated by an external magnetic field [6–12]. In addition to this, high surface area, high activity, surface modification ability, catalyst recovery, excellent thermal and chemical stability, possibility of re-use of catalysts, are ideal properties of “green catalysts”.

Therefore, the design of novel MCRs used by nanocatalysts for the synthesis of complex organic compounds has remained an important topic for medicinal and organic chemistry. Having xanthen and 3-aminoisoxazole moieties, Heterocycles are significant targets in synthetic organic chemistry. Benzoxanthenes and isoxazole derivatives are popular scaffolds for the development of new agents with variable biological activities, such as anti-microbial, anti-viral, anti-cancer, immunomodulatory, and anti-diabetic properties [13–17].

Here, we demonstrate an important finding in which that isolated Fe<sub>3</sub>O<sub>4</sub> nanoparticles can be stabilized by THAM, which is inexpensive, readily available and has many applications in medicine, biochemistry, and biology. Clearly, the production of THAM-stabilized nanoparticles [18, 19] is environmentally friendly, and thioglycolic acid is used as a chemical depilatory especially in salt forms, including calcium thioglycolate and sodium thioglycolate. This nanocatalyst is used as an acidity indicator.

In continuation of our interest in the heterocyclic system and magnetic nanoparticles [20–22], herein we report the preparation of a novel acidic nanocatalyst and its application for the green synthesis of 3-amino isoxazolmethylnaphthol and 12-aryl-8,9,10,12-tetrahydrobenzo[*a*]xanthen-11-one derivatives (Scheme 1).

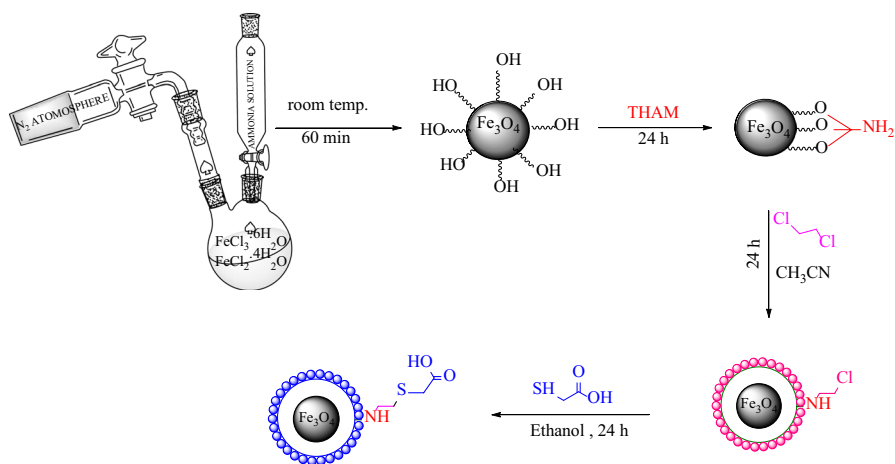
The reaction involves one-pot, three-components coupling of 2-naphthol **1**, benzaldehyde **2**, and 3-amino-5-methylisoxazole **3** or dimedone **5** in the presence of  $\text{Fe}_3\text{O}_4@\text{THAM-CH}_2\text{CH}_2\text{-SCH}_2\text{CO}_2\text{H}$  as a new, efficient, and non-toxic catalyst under solvent-free condition. All reactions proceeded with good to excellent yields in a short time, and the catalyst could be used up to eight times without significant loss of its activity.

## Result and discussion

### Preparation and characterization of THAM- $\text{CH}_2\text{CH}_2\text{-SCH}_2\text{CO}_2\text{H}$ coated core-shell magnetic nanocatalyst

In this study,  $\text{Fe}_3\text{O}_4$  MNPs were prepared through a common precipitation method in r.t., for hosting THAM active species and forming  $\text{Fe}_3\text{O}_4@\text{THAM}$  NPs. To immobilize thio glycolic acid on to the magnetic core, first, the  $\text{Fe}_3\text{O}_4$  NPs have modified with THAM magnetic NPs. In the next step, the interaction between the 1,2-dichloro ethane and the surface OH groups of the MNP derived effective attachment  $\text{Fe}_3\text{O}_4@\text{THAM-CH}_2\text{CH}_2\text{Cl}$  and then thio glycolic acid was coated (Scheme 2).

Synthesized pure  $\text{Fe}_3\text{O}_4$  MNPs and  $\text{Fe}_3\text{O}_4@\text{THAM-CH}_2\text{CH}_2\text{-SCH}_2\text{CO}_2\text{H}$  nanocatalyst were characterized using powder XRD, FE-SEM, TEM, FT-IR, VSM. Elemental analysis results indicate the presence of sulfur and nitrogen confirming the THAM coating on the surface  $\text{Fe}_3\text{O}_4$ .



**Scheme 2** Preparation of THAM- $\text{CH}_2\text{CH}_2\text{-SCH}_2\text{CO}_2\text{H}$  coated core-shell magnetic nanocatalyst

## FT-IR

FT-IR spectra of the prepared  $\text{Fe}_3\text{O}_4$  MNPs and MNPs- $\text{CO}_2\text{H}$  are shown in Fig. 1. There are several vibrational peaks in the spectrum of the  $\text{Fe}_3\text{O}_4$  NPs that verify the  $\text{Fe}_3\text{O}_4$  structure. These peaks include the 1618 and  $3374\text{ cm}^{-1}$  broad bands, which refer to the surface-adsorbed water molecules and hydroxyl groups, and the 582 and  $631\text{ cm}^{-1}$  peaks associated with the octahedral bending and tetrahedral stretching modes of the Fe–O functional group. Based on Fig. 1, the FT-IR peaks of C–Cl and CH–Cl are positioned at 780,  $1200\text{ cm}^{-1}$ . On the other hand, the absorption peak around 2923 indicated C–H stretching vibrations in the aliphatic group [18]. Finally, the presence of thioglycolic acid is confirmed by 3392, 1601, 1411, 1035 peaks. With respect to the FT-IR spectra, the surface of  $\text{Fe}_3\text{O}_4$  NPs is successfully coated by THAM, 1,2-dichloroethane and thioglycolic acid.

## XRD

XRD diffraction patterns of undoped  $\text{Fe}_3\text{O}_4$  and thioglycolic acid doped  $\text{Fe}_3\text{O}_4$  nanocatalyst are shown in Fig. 2. The powder XRD patterns of  $\text{Fe}_3\text{O}_4$  and  $\text{Fe}_3\text{O}_4$ @THAM- $\text{CH}_2\text{CH}_2$ @ $\text{SCH}_2\text{CO}_2\text{H}$  MNPs exhibited diffraction peaks at  $2\theta = 30.34^\circ$ ,  $35.65^\circ$ ,  $36.99^\circ$ ,  $43.12^\circ$ ,  $53.56^\circ$ ,  $57.11^\circ$ , and  $62.56^\circ$ , which are associated with corresponding indicants of (2 2 0), (3 1 1), (2 2 2), (4 0 0), (4 2 2), (5 1 1), and (4 4 0), respectively [18]. The XRD pattern of  $\text{Fe}_3\text{O}_4$ @THAM- $\text{CH}_2\text{CH}_2$ @ $\text{SCH}_2\text{CO}_2\text{H}$  MNPs showed a broad band less than  $20^\circ$  that can be related to the amorphous layer

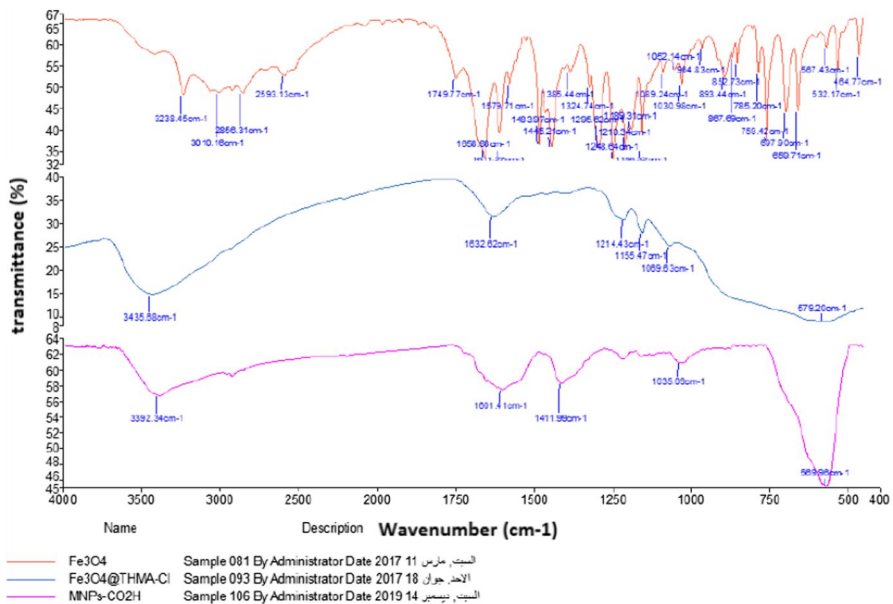
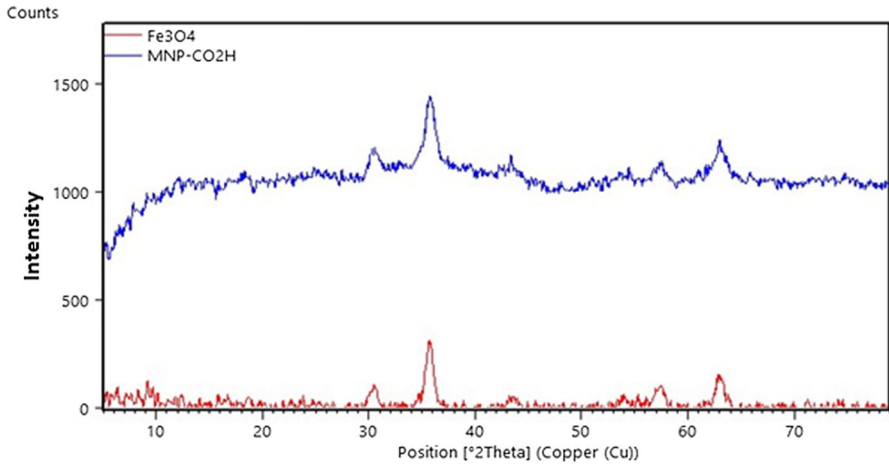


Fig. 1 FT-IR spectra of  $\text{Fe}_3\text{O}_4$  (a)  $\text{Fe}_3\text{O}_4$ @THAM-Cl (b), and MNPs- $\text{CO}_2\text{H}$  (c)



**Fig. 2** XRD pattern of  $\text{Fe}_3\text{O}_4$  (a) and MNPs– $\text{CO}_2\text{H}$  (b)

including thioglycolic acid. The crystallite sizes of nanocatalyst can be calculated by the Scherrer’s formula. Therefore, the average crystallite sizes of nanocatalyst were calculated to be 13.70382, and lattice constants were a (Å):8.3100, b (Å): 8.3100, c (Å): 8.3100, Alpha (°): 90.0000, Beta (°):90.0000, Gamma (°): 90.0000 with Reference code:01-075-0449 in Crystal system:Cubic. D-spacing can be calculated by Bragg law. The results are summarized in Table 1.

**TGA**

Thermogravimetry indicates that the mass loss at 160 °C is the mass of the molecular water in the catalyst. The organic moiety grafted on the  $\text{Fe}_3\text{O}_4$  NPs decomposed in the temperature range of 180–600 °C (5.38%). In accordance with this mass loss, the amount of 53.8 mg (0.22 mmol) of the organic layer was loaded on 1 g of  $\text{Fe}_3\text{O}_4$

**Table 1** d-spacing of nanocatalyst

Entry	h	k	l	d [Å]	2Theta [°]	I [%]
1	1	1	1	4.79778	18.478	6.9
2	2	2	0	2.93803	30.399	28.7
3	3	1	1	2.50556	35.810	100.0
4	2	2	2	2.39889	37.460	7.5
5	4	0	0	2.07750	43.528	19.8
6	3	3	1	1.90644	47.663	1.1
7	4	2	2	1.69627	54.016	7.8
8	5	1	1	1.59926	57.588	23.7
9	4	4	0	1.46901	63.251	32.9
10	5	3	1	1.40465	66.514	0.6

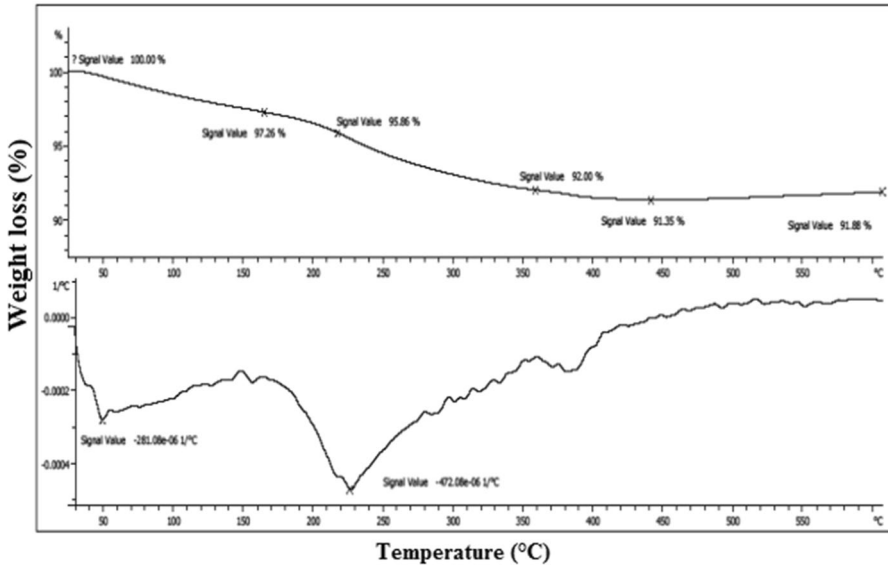


Fig. 3 Thermogravimetry (TGA) of Synthesized MNPs-CO<sub>2</sub>H

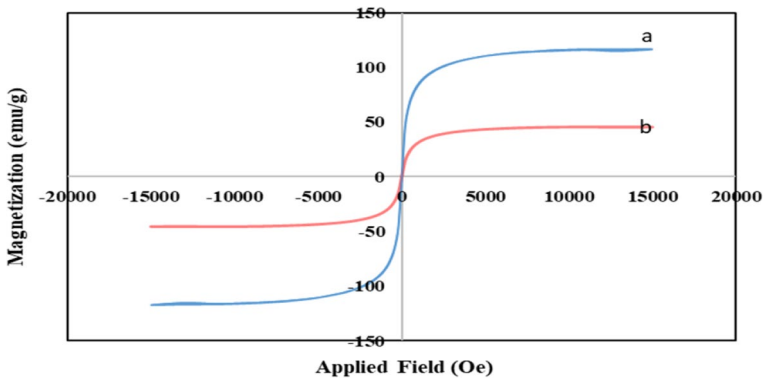


Fig. 4 Comparison of pure magnetic properties of synthesized Fe<sub>3</sub>O<sub>4</sub> MNPs (a) and MNPs-CO<sub>2</sub>H (b)

nanoparticles. Furthermore, the DTG curve indicates that the nanocatalyst has good thermal stability before 230 °C (Fig. 3).

## VSM

Variation of pure magnetic properties of synthesized Fe<sub>3</sub>O<sub>4</sub> MNPs and MNPs-CO<sub>2</sub>H was investigated using VSM at room temperature with an applied field of 15,000 Oe. As VSM indicates, both samples exhibit the typical behavior of superparamagnetic materials and give nearly zero coercivity and remanence. Moreover, according to Fig. 4, the nonmagnetic coating including THAM and thioglycolic acid

species decreases the amount of saturation magnetization ( $M_s$ ) of the final MNPs (about  $55 \text{ emu g}^{-1}$ ) than magnetization value of bulk (about  $116 \text{ emu g}^{-1}$ ).

### TEM, FE-SEM, and EDS

TEM and SEM images were performed to examine the morphology, size distribution, and physical properties of synthesized nanoparticles. As can be seen in Fig. 5, the MNPs have nano-size with spherical morphology. In addition, the EDS study was used to confirm the presence of thioglycolic acid and shell extract on the surface of the species  $\text{Fe}_3\text{O}_4\text{NPs}$  (Fig. 6).

### Synthesis of 3-aminoisoxazolmethylnaphthols

In order to investigate the optimizing reaction conditions for the synthesis of functionalized 3-aminoisoxazole, we carried out the multi-component reaction between 2-naphthol (1.0 mmol), benzaldehyde (1.0 mmol) and 3-amino-5-methylisoxazole (1.0 mmol) as a model (Scheme 3). For characterization of solvents, initially, the model reaction was studied using various green solvents and solvent-free conditions. All of the results are registered in Table 2. Among the investigated solvents (EtOH,  $\text{H}_2\text{O}$ , and AcOH with yields including 56, 66, and 54%), the solvent-free condition showed the strongest effect and the highest yield (95%) on the model reaction (Table 2, entry 1). Then, the effect of amount of catalyst was investigated, and the highest yield of target product was obtained using 0.01 g of catalyst (Table 3, entry 1). Finally, the effect of temperature was studied. Based on our experimental results (Table 3), the best conversion was obtained at  $80^\circ\text{C}$  in the presence of 0.01 g of MNPs- $\text{CO}_2\text{H}$ , which is an efficient condition (Table 3, entry 1). Also,

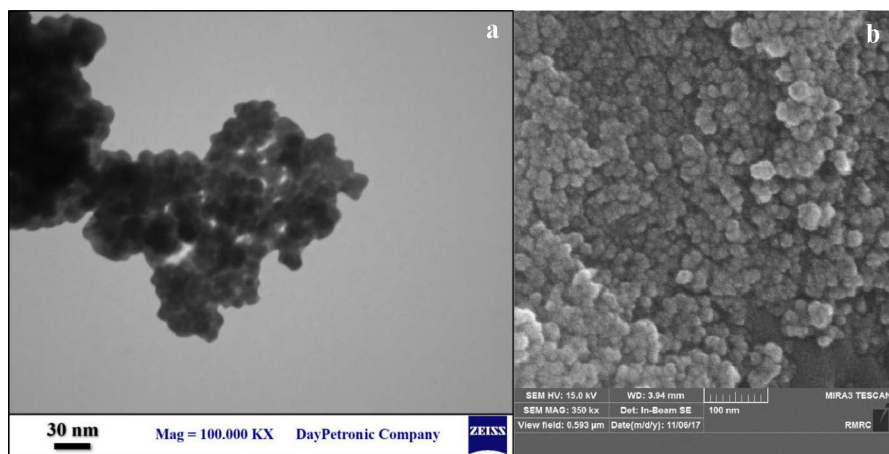
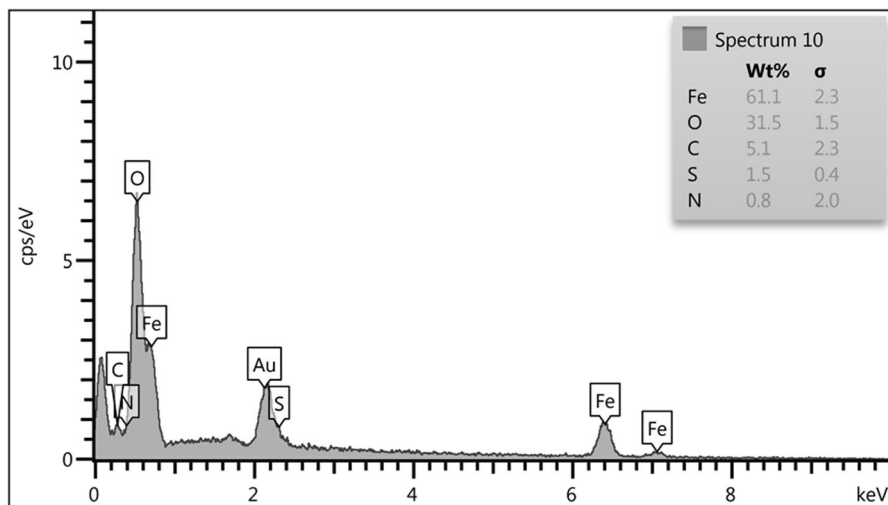
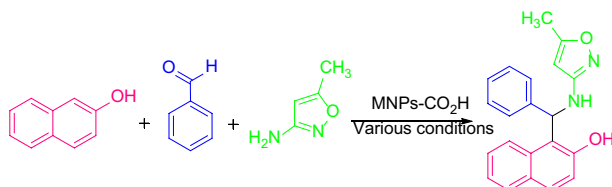


Fig. 5 TEM (a) and SEM (b) images of MNPs- $\text{CO}_2\text{H}$

Fig. 6 EDS for MNPs-CO<sub>2</sub>H

**Scheme 3** Synthesis of 1-((5-methylisoxazol-3-yl) amino) (phenyl)methyl naphthalen-2-ol under various conditions as a model reaction

**Table 2** Investigation of solvent effects on the reaction

Entry	Solvent	Temp. (°C)	Time (min)	Yield%
1	Solvent-free	80	5	95
2	Ethanol	80	40	56
3	ACOH	80	55	54
4	H <sub>2</sub> O	80	40	66

**Table 3** Optimization of the catalyst value and reaction temperature in the desired reaction

Entry	Amount of catalyst (gr)	Temp. (°C)	Time (min)	Yield (%)
1	0.01	80	5	95
2	0.02	80	4	89
3	0.01	25	60	Trace
4	0.01	50	55	52
5	0.01	70	15	78
6	0.01	90	3	86

Further enlarge the scope of these conditions, we conducted reaction with a variety of substituted aldehydes under the optimized condition for the synthesis of 3-aminoisoxazolumethylnaphthols (**4a-l**). There is smooth progression in reaction for various substituents to afford the products in high yields. The obtained results are summarized in (Table 4).

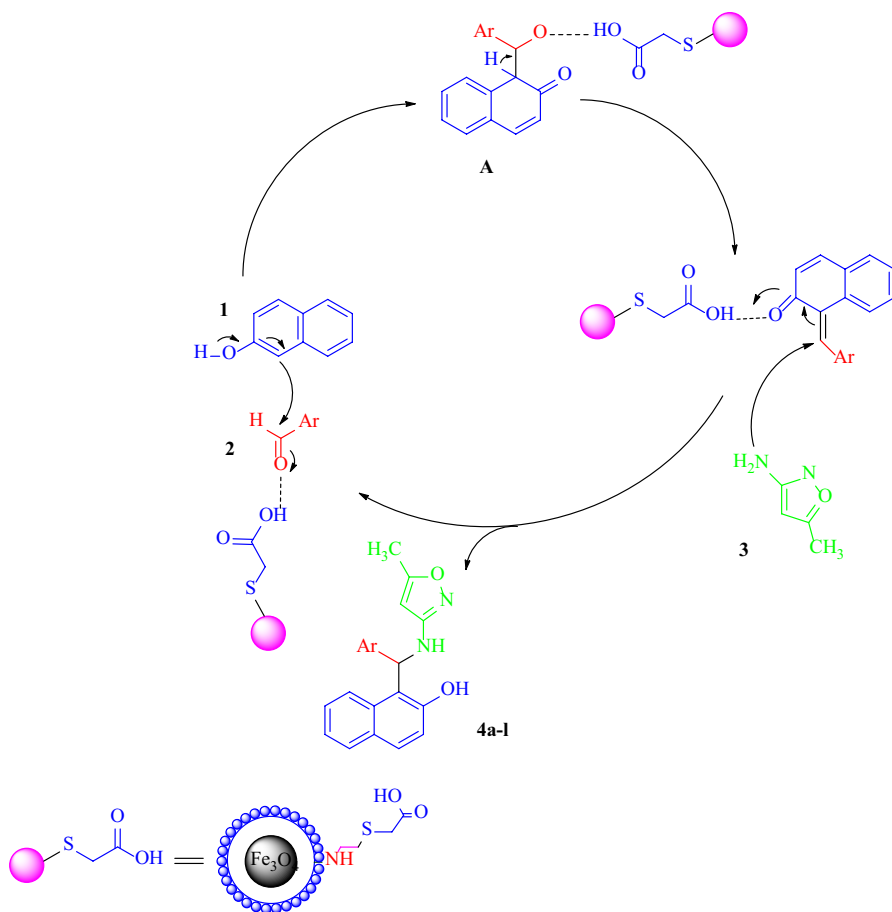
Nanocatalysts are attractive alternatives to conventional catalysts because when the size of the material is decreased to the nanometer scale, the surface area is significantly increased, and the catalyst can be equally dispersed in solution, to form a homogenous emulsion. A possible mechanism for the synthesis of 3-aminoisoxazolumethylnaphthol derivatives **4** using MNPs-CO<sub>2</sub>H outlined in Scheme 4 acts as a heterogeneous catalysis in all steps. In this mechanism, MNPs-CO<sub>2</sub>H is an efficient catalyst to form the olefin **A**, which readily prepares in situ from Knoevenagel condensation of aromatic aldehyde **2** with 2-naphthol **1**. The Michael addition of 3-amino-5-methyl isoxazole **3** with olefin **A** in the presence of MNPs-CO<sub>2</sub>H then causes the inner molecular ring to be formed after a tautomeric proton shift to produce the corresponding products **4a-l**.

### Produce of 12-aryl-8,9,10,12-tetrahydrobenzo[*a*]xanthen-11-one derivatives

The catalytic performance of MNPs-CO<sub>2</sub>H was tested in one-pot, three-component reaction of 2-naphthol **1** (1.0 mmol), benzaldehyde **2** (1.0 mmol) dimedone **5** (1.0 mmol) as a model reaction (Scheme 5). At the outset, a test reaction was accomplished in the presence of 0.005 g of catalyst at 50 °C and offered 94% yield of the desired product, as shown in (Table 5, entry1). Then, for characterization of solvents, a brief screening of diverse green solvents (EtOH, H<sub>2</sub>O, and AcOH) was afforded (Table 5). These studies revealed that the rate solvent-free is better than other rates. Finally, to investigate the efficacy of reaction temperature, the model reaction was

**Table 4** Synthesis of 3-aminoisoxazolumethylnaphthols in the presence of MNPs- MNPs-CO<sub>2</sub>H under solvent-free conditions at 80 °C

Entry	Derivatives	Time (min)	Yield (%)	Product	m.p. obs. (°C)	m.p lit. (°C)
1	H	5	95	<b>4a</b>	212–213	212–214 [22]
2	4-Me	10	89	<b>4b</b>	202–203	202–203 [23]
3	4-OMe	13	86	<b>4c</b>	193–194	194–195 [23]
4	4-Cl	6	93	<b>4d</b>	192–193	194–195 [23]
5	3-Cl	4	90	<b>4e</b>	192–193	193–195 [23]
6	2-Cl	6	89	<b>4f</b>	186–187	185–186 [23]
7	4- Br	4	96	<b>4g</b>	198–199	200–201 [23]
8	3-Br	5	95	<b>4h</b>	193–194	195–196 [23]
9	4-F	6	90	<b>4i</b>	192–193	193–194 [23]
10	4-NO <sub>2</sub>	11	91	<b>4j</b>	149–150	150–151 [23]
11	3-NO <sub>2</sub>	13	92	<b>4k</b>	146–147	148–150 [23]
12	2-NO <sub>2</sub>	14	86	<b>4l</b>	147–148	149–150 [23]



**Scheme 4** Possible mechanism for the synthesis of 3-aminoisoxazolinemethylnaphthol in the presence of MNP-CO<sub>2</sub>H

done at different temperatures. The yield growth to 94% when the reaction was carried out at 50 °C temperature (Table 6, entry 1).

After broad screening, we found the best optimized yields and time profiles with 0.005 g of MNPs-CO<sub>2</sub>H at 50 °C under solvent-free conditions, which furnished the corresponding 9,9-dimethyl-12-phenyl-9,10-dihydro-8*H*-benzo[*a*]xanthen-11(12*H*)-one **6a** in 94% yield within 4 min proceed efficiently. The results are summarized in Tables 5, 6, and 7.

Using these optimized reaction conditions, the scope and efficiency of the reaction were explored for the synthesis of a wide variety of 12-aryl-8,9,10,12-tetrahydrobenzo[*a*]xanthen-11-one derivatives. The results are summarized in Table 7.

A proposed mechanism for the synthesis of 12-aryl-8,9,10,12-tetrahydrobenzo[*a*]xanthen-11-one derivatives is illustrated in Scheme 6. We suggest that intermediate

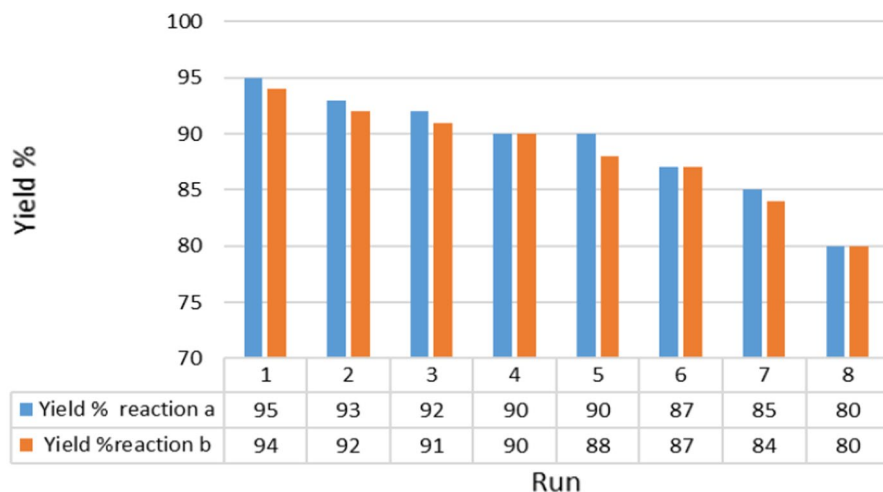
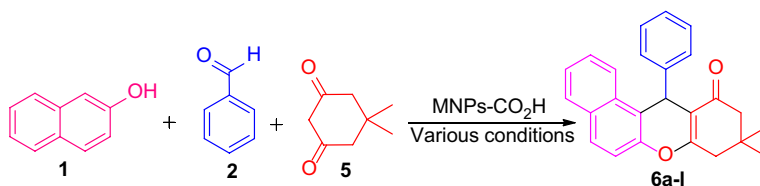


**Fig. 7** Recovery of MNPs- CO<sub>2</sub>H in the synthesis of 3-aminoisoxazomethylnaphthols (a) and 12-aryl-8,9,10,12-tetrahydrobenzo[a]xanthen-11-one (b)



**Scheme 5** Production of 9,9-dimethyl-12-phenyl-9,10-dihydro-8H-benzo[a]xanthen-11(12H)-one

**Table 5** Investigation of solvent effects on the reaction

Entry	Solvent	Temp. (°C)	Time (min)	Yield (%)
1	Solvent-free	50	4	94
2	Ethanol	50	20	75
3	ACOH	50	40	65
4	THF	50	45	60

**Table 6** Optimization of the catalyst value and reaction temperature for the desired reaction

Entry	Amount of catalyst (g)	Temp. (°C)	Time (min)	Yield (%)
1	0.005	50	4	94
2	0.01	50	3	85
3	0.005	r.t	50	78
4	0.005	60	5	80
5	0.005	80	5	83
6	0.005	90	4	85

**Table 7** Production of 12-aryl-8,9,10,12-tetrahydrobenzo[*a*]xanthen-11-one derivatives in the presence MNPs-CO<sub>2</sub>H under solvent-free conditions at 50 °C

Entry	Derivatives	Time (min)	Yield %	Product	m.p. (°C)	m.p. ref. (°C)
1	H	4	94	<b>6a</b>	148–149	149–151 [24]
2	4-Me	9	91	<b>6b</b>	174–175	176–177 [24]
3	4-OMe	11	89	<b>6c</b>	200–201	203–205 [24]
4	4-Cl	6	94	<b>6d</b>	172–173	173–174 [25]
5	2,4-Di Cl	9	92	<b>6e</b>	173–174	175–176 [26]
6	2-Cl	7	91	<b>6f</b>	171–172	173–174 [26]
7	3-OH	13	94	<b>6g</b>	239–240	240–241 [27]
8	2-OH 5-Br	10	92	<b>6h</b>	265–266	266–268 [27]
9	4-F	5	91	<b>6i</b>	175–176	177–180 [25]
10	4-NO <sub>2</sub>	8	90	<b>6j</b>	176–177	176–178 [24]
11	3-NO <sub>2</sub>	9	89	<b>6k</b>	166–167	168–169 [24]
12	2-NO <sub>2</sub>	14	88	<b>6l</b>	218–219	218–220 [24]

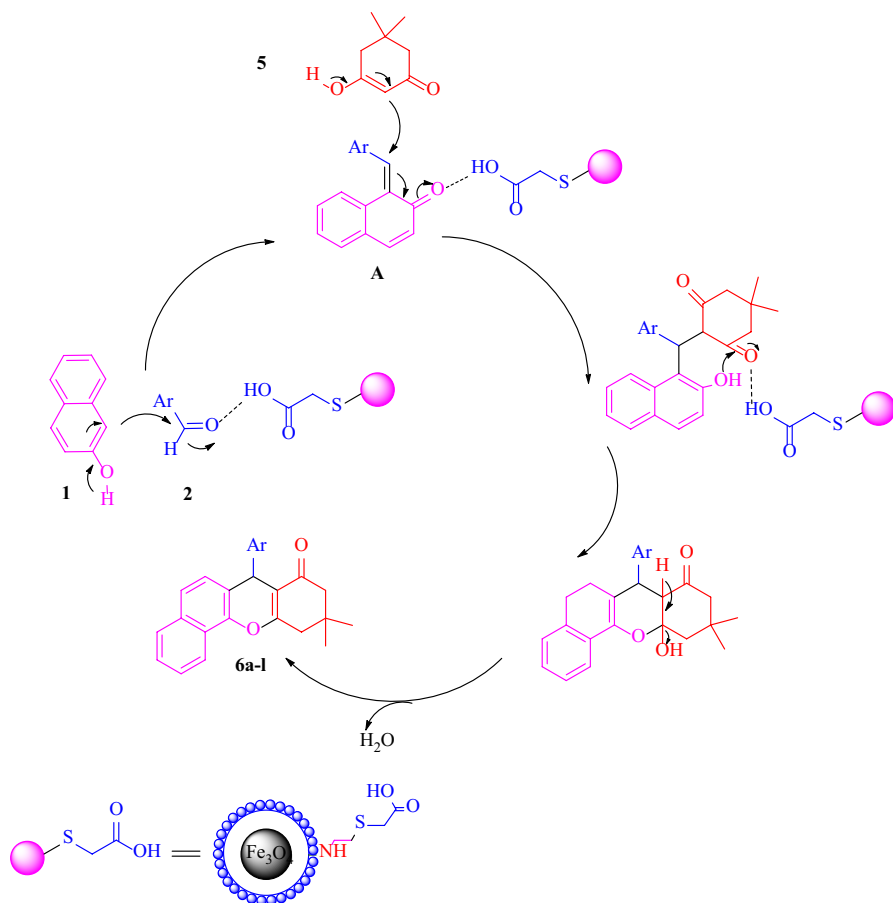
(**A**) be created by the nucleophilic addition of 2-naphthol to the activated benzaldehyde, facilitated by proton of MNP-CO<sub>2</sub>H. Intermediate (**A**) react with dimedone via Michael addition and then eliminate one molecule of H<sub>2</sub>O to close the ring and obtain the products **6a-l**. The role of the catalyst depends on CO<sub>2</sub>H-functionalized active sites, which might exhibit excellent catalytic activity in rapid transfer of protons.

### Recycling experiments of the nanocatalyst

After completion of the reaction, the resulting product was dissolved with hot ethanol, and the catalyst was easily separated by an external magnet. To eliminate impurities, the product was crystallized in ethanol. The catalyst was separated from the reaction mixture using an external magnet, and it was washed with ethanol (2 × 5 mL) to remove any unreacted organic compound. The washed catalyst was dried in an oven at 70 °C for the cycle of reaction. The same purification procedure of the catalyst was carried out after each catalytic cycle. Interestingly, for up to five cycles of reaction, no loss of activity of the catalyst was observed. The catalytic activity was found to decrease to a small extent from the sixth cycle, and after the eighth cycle, the yield was 80% that may be due to little weight loss of catalyst during each recovery process (Fig. 7).

### Comparison between present reaction methodology and previously reported methods

Many methods have been reported for the synthesis of 12-aryl-8,9,10,12-tetrahydrobenzo[*a*]xanthen-11-one and 3-aminoisoxazolmethyl-naphthol derivatives from the reaction of benzaldehyde, 2-naphthol, and dimedone or and 3-amino-5-methylisoxazole (Table 8). This methods offer disadvantages such as high temperature



**Scheme 6** Synthesis of 12-aryl-8,9,10,12-tetrahydrobenzo[*a*]xanthen-11-one derivatives with using MNP-CO<sub>2</sub>H

(entry 1, 3, 6, 7, 8), long reaction times (entry 5, 10), hard reaction conditions (entry 10), but in present work, the Fe<sub>3</sub>O<sub>4</sub> nanoparticles (NPs) was synthesized easily by chemical coprecipitation method at room temperature. The synthesis of Fe<sub>3</sub>O<sub>4</sub> NPs at room temperature has some advantage such as better magnetic properties and avoids Fe<sub>3</sub>O<sub>4</sub> to  $\gamma$ -Fe<sub>2</sub>O<sub>3</sub> conversion. This method offers some advantages in terms of solvent-free condition, short reaction times, mild reaction conditions and excellent yields and utilization of a reusable catalyst, eco-friendly nature that make it sustainable, attractive and economic in agreement with some green chemistry protocols.

## Conclusion

A mild and efficient method has been developed to promote the synthesis of 3-amino isoxazolmethylnaphthol and 12-aryl-8,9,10,12-tetrahydrobenzo[*a*]xanthen-11-one

**Table 8** Comparison between this work and previously reported methods

Entry	Product	Catalyst	Time (min)	Temp (°C)	Yield (%)	Ref.
1	<b>4a</b>	Oxalic acid	8	90	92	[23]
2	<b>4a</b>	Fe <sub>3</sub> O <sub>4</sub> -NHPhSO <sub>3</sub> H	8	70	93	[38]
3	<b>6a</b>	SrFe <sub>12</sub> O <sub>19</sub>	15	80	98	[36]
4	<b>6a</b>	γ-Fe <sub>2</sub> O <sub>3</sub> [Fe <sub>2</sub> O <sub>3</sub> @HAp]	4	60	96	[35]
5	<b>6a</b>	Fe <sub>3</sub> O <sub>4</sub> @chitosan	180	40	90	[37]
6	<b>6a</b>	AIL@MNP	40	90	91	[33]
7	<b>6a</b>	Fe <sub>3</sub> O <sub>4</sub> /CS-Ag NPs	30	80	95	[32]
8	<b>6a</b>	LAIL@MNP	30	80	96	[34]
9	<b>6a</b>	Iodine	60	60	90	[29]
10	<b>6a</b>	NaHSO <sub>4</sub> ·SiO <sub>2</sub>	300	Reflux	87	[30]
11	<b>6a</b>	Lactic Acid	30–40	50	95	[31]
12	<b>6a</b>	Trityl chloride	40–70	110	89	[28]

derivatives employing a magnetically separable core-shell Fe<sub>3</sub>O<sub>4</sub>@THAM-CH<sub>2</sub>CH<sub>2</sub>-SCH<sub>2</sub>CO<sub>2</sub>H nanocatalyst under solvent-free conditions. Several useful favorites, such as short time reaction, easy workup, good to excellent yields of products, and use of a magnetically separable and recyclable nano catalyst, make this method attractive. To the best of our knowledge, this is the first report of the synthesis of a core-shell structured MNPs-CO<sub>2</sub>H nanocatalyst and its successful application as an efficient heterogeneous acid catalyst.

## Experimental

### General

Solvents and chemicals were purchased from commercial suppliers and used without further purification. Melting points were measured in open capillary tubes and were uncorrected. Melting points and IR spectra of all compounds were determined by using an Electrothermal 9100 apparatus and a PerkinElmer plus a spectrometer. The <sup>1</sup>H and <sup>13</sup>C NMR spectra of known compounds were recorded on a Bruker DRX-400 Avance instrument in CDCl<sub>3</sub> and DMSO at 300 and 400 MHz. MNPs-CO<sub>2</sub>H nanocatalyst was characterized by methods like this: FT-IR, TEM, VSM, XRD, TGA, FE-SEM, and EDS.

### Catalyst preparation

#### Synthesis of Fe<sub>3</sub>O<sub>4</sub> magnetite nanoparticles

MNPs-CO<sub>2</sub>H nanocatalyst was synthesized using a four-step approach. At the first, the mixture of FeCl<sub>3</sub>·6H<sub>2</sub>O (10.0 mmol) and FeCl<sub>2</sub>·4H<sub>2</sub>O (5.0 mmol) was dissolved

in 100 mL deionized water at room temperature. Then, a solution of ammonia was added dropwise to medium reaction until  $\text{pH} = 11$ . The black suspension was stirred for 1 h in nitrogen atmosphere. Finally, nanoparticles (MNPs) were isolated by an external magnet. MNPs were washed with water and ethanol and dried in an oven for 2 h at  $80\text{ }^\circ\text{C}$ .

### Synthesis of $\text{Fe}_3\text{O}_4\text{@THAM}$

In the next step,  $\text{Fe}_3\text{O}_4\text{@THAM}$  MNPs was prepared by dispersing  $\text{Fe}_3\text{O}_4$  MNPs (1.0 g) in the presence of 40 mL water and 60 mL ethanol for 30 min, then 2.0 g of tris(hydroxymethyl) aminomethane was added in  $\text{N}_2$  atmosphere and reflux condition for 24 h. Similar to the previous step, MNPs were gathered, washed, and dried at  $80\text{ }^\circ\text{C}$ .

### Synthesis of $\text{Fe}_3\text{O}_4\text{@THAM-CH}_2\text{CH}_2\text{Cl}$

Next,  $\text{Fe}_3\text{O}_4\text{@THAM}$  was dispersed in 50 mL of acetonitrile. Then, 1 mL of dichloroethane and 0.1 mL of triethylamine were added to the mixture of reaction under reflux condition, and the resulting mixture was refluxed under  $\text{N}_2$  atmosphere for 24 h to produce  $\text{Fe}_3\text{O}_4\text{@THAM-CH}_2\text{CH}_2\text{Cl}$  MNPs. These nanoparticles were cooled to room temperature, washed with water/ethanol, separated using an external magnet, and dried at  $80\text{ }^\circ\text{C}$ .

### Synthesis of $\text{Fe}_3\text{O}_4\text{@THAM-CH}_2\text{CH}_2\text{-SCH}_2\text{CO}_2\text{H}$

Finally, MNP levels of  $\text{Fe}_3\text{O}_4\text{@THAM-CH}_2\text{CH}_2\text{Cl}$  were functionalized by dispersing them in 100 mL of ethanol using an ultrasonic bath for 30 min and reacting with 1.5 mL thioglycolic acid. The mixture was mechanically stirred under reflux condition and  $\text{N}_2$  atmosphere for 24 h, it was cooled at room temperature and was washed with water/ethanol and dried at  $80\text{ }^\circ\text{C}$  for 8 h for desired  $\text{Fe}_3\text{O}_4\text{@THAM-CH}_2\text{CH}_2\text{-SCH}_2\text{CO}_2\text{H}$  preparation. Synthesized MNPs- $\text{CO}_2\text{H}$  was characterized by infrared spectroscopy (FT-IR), field emission scanning electron microscopy (FE-SEM), energy dispersive X-ray spectroscopy (EDS), transmission electron microscopy (TEM), and vibrating sample magnetometry (VSM).

### General experimental procedure for the preparation of 3-aminoisoxazolmethyl-naphthols

Initially, the reactants of benzaldehyde (1.0 mmol) and 2-naphthol (1.0 mmol), 3-amino-5-methylisoxazole (1.0 mmol), and 0.01 g of MNPs- $\text{CO}_2\text{H}$  were stirred at  $80\text{ }^\circ\text{C}$  under solvent-free conditions. After completion of the reaction mentioned by TLC, the reaction mixture was cooled to room temperature and washed with 5 mL of water to separate the product. The resulting mixture was diluted with hot ethanol, and the catalyst was easily separated by an external magnet. To eliminate impurities, the product was crystallized in ethanol.

## General experimental procedure for the synthesis of 12-aryl-8,9,10,12-tetrahydrobenzo [a]xanthen-11-one derivatives

In a test tube, benzaldehyde (1.0 mmol), dimedone (1.0 mmol), 2-naphthol (1.0 mmol), and MNPs-CO<sub>2</sub>H nanoparticles (0.005 g) were added at 50 °C for the desired time. After completion of the reaction (the reaction mixture was monitored using TLC), the reaction mixture was diluted with hot ethanol, and the catalyst was easily separated from the reaction mixture by an external magnet, washed with hot ethanol, dried and reused for a consecutive run under the same reaction conditions. Then, the reaction mixture was cooled to room temperature, and the obtained crude product was collected by filtration and recrystallized from hot ethanol to give the pure solid **6a**.

### Spectral data for the selected compounds

#### 1-[(5-Methyl-isoxazol-3-ylamino)-phenyl-methyl]-naphthalen-2-ol (4a)

IR (KBr  $\nu_{\max}$ , cm<sup>-1</sup>): 3403, 3058, 2925, 1628, 1600, 1581, 1541, 1516, 1493. <sup>1</sup>H NMR (300 MHz, DMSO-d<sub>6</sub>): 10.10 (1H, s, OH), 8.03 (1H, d, NH, J=8.1 Hz), 7.76–7.83 (2H, m, H<sub>aromat</sub>), 7.14–7.41 (8H, m, H<sub>aromat</sub>), 6.79 (2H, dd, H<sub>aromat</sub>, J=26.2 Hz, J=7.5 Hz), 5.90 (1H, s, CHNH), 2.23 (3H, s, CH<sub>3</sub>).

#### 1-[(4-Methoxy-phenyl)-(5-methyl-isoxazol-3-ylamino)-methyl]-naphthalen-2-ol (4c)

<sup>1</sup>H NMR (300 MHz, DMSO-d<sub>6</sub>): 10.06 (1H, s, OH), 8.00 (1H, d, NH), 7.73–7.81 (2H, m, H<sub>aromat</sub>), 7.20–7.39 (4H, m, H<sub>aromat</sub>), 6.76–6.85 (3H, m, H<sub>aromat</sub>), 6.64 (1H, d, H<sub>aromat</sub>, J=5.7 Hz), 5.86 (1H, s, CHNH), 3.69 (3H, s, OCH<sub>3</sub>), 2.21 (3H, s, CH<sub>3</sub>).

#### 1-[(4-Chloro-phenyl)-(5-methyl-isoxazol-3-ylamino)-methyl]-naphthalen-2-ol (4d)

<sup>1</sup>H NMR (300 MHz, DMSO-d<sub>6</sub>): 2.23 (3H, s, CH<sub>3</sub>), 5.88 (1H, s, CHNH), 6.79 (2H, dd, H<sub>aromat</sub>, J=49.2 Hz, J=6.9 Hz), 7.25–7.42 (7H, m, H<sub>aromat</sub>), 7.80 (2H, t, H<sub>aromat</sub>, J=9 Hz), 7.97 (1H, d, NH, J=7.8 Hz), 10.16 (1H, s, OH); <sup>13</sup>C NMR (75 MHz, DMSO-d<sub>6</sub>): 167.8, 164.9, 153.2, 142.8, 132.5, 130.9, 129.8, 129.0, 128.5, 128.3, 126.8, 124.0, 122.9, 119.9, 118.8, 94.4, 52.5, 12.5.

#### 1-[(3-Chloro-phenyl)-(5-methyl-isoxazol-3-ylamino)-methyl]-naphthalen-2-ol (4e)

<sup>1</sup>H NMR (300 MHz, DMSO-d<sub>6</sub>): 10.16 (1H, s, OH), 7.99 (1H, d, NH, J=8.1 Hz), 7.78–7.84 (1H, t, H<sub>aromat</sub>), 7.39–7.44 (1H, t, H<sub>aromat</sub>), 7.19–7.34 (6H, m, H<sub>aromat</sub>), 6.81 (2H, dd, H<sub>aromat</sub>, J=46.2 Hz, J=7.2 Hz), 5.88 (1H, s, CHNH), 2.23 (3H, s, CH<sub>3</sub>); <sup>13</sup>C NMR (75 MHz, DMSO-d<sub>6</sub>): 167.9, 164.8, 153.2, 146.5, 133.2, 132.4,

130.3, 129.9, 129.0, 126.9, 126.4, 126.3, 125.4, 123.8, 122.9, 119.8, 118.8, 94.4, 52.6, 12.5.

#### 1-[(2-2.3.6.1-[(3-Chloro-phenyl)-(5-methyl-isoxazol-3-ylamino)-methyl]-naphthalen-2-ol (4f)

$^1\text{H}$  NMR (300 MHz, DMSO- $d_6$ ): 2.22 (3H, s,  $\text{CH}_3$ ), 5.78 (1H, s, CHNH), 6.83 (2H, dd,  $H_{\text{aromat}}$ ,  $J=46.5$ ,  $J=5.7$ ), 7.16–7.42 (6H, m,  $H_{\text{aromat}}$ ), 7.69–7.82 (2H, m,  $H_{\text{aromat}}$ ), 8.06 (1H, d, NH,  $J=8.70$  Hz), 9.94 (1H, s, OH);  $^{13}\text{C}$  NMR (75 MHz, DMSO- $d_6$ ): 168.2, 163.6, 154.2, 146.5, 134.2, 132.4, 130.3, 129.9, 129.5, 129.2, 126.9, 126.4, 126.5, 125.4, 123.6, 122.9, 120.0, 118.6, 94.4, 52.5, 12.5.

#### 1-[(4-Bromo-phenyl)-(5-methyl-isoxazol-3-ylamino)-methyl]-naphthalen-2-ol (4 g)

$^1\text{H}$  NMR (300 MHz, DMSO- $d_6$ ): 10.16 (1H, s, OH), 7.97 (1H, d, NH,  $J=8.1$  Hz), 7.77–7.83 (2H, t,  $H_{\text{aromat}}$ ), 7.23–7.48 (7H, m,  $H_{\text{aromat}}$ ), 6.77 (2H, dd,  $H_{\text{aromat}}$ ,  $J=6.6$  Hz,  $J=48.9$  Hz), 5.88 (1H, s, CHNH), 2.23 (3H, s,  $\text{CH}_3$ );  $^{13}\text{C}$  NMR (75 MHz, DMSO- $d_6$ ): 167.8, 164.9, 153.2, 143.3, 132.9, 131.2, 129.8, 129.0, 128.9, 126.8, 124.0, 122.9, 119.9, 119.4, 118.8, 94.4, 52.6, 12.5.

#### 1-[(3-Bromo-phenyl)-(5-methyl-isoxazol-3-ylamino)-methyl]-naphthalen-2-ol (4 h)

$^1\text{H}$  NMR (300 MHz, DMSO- $d_6$ ): 10.14 (1H, s, OH), 7.99 (1H, d, NH,  $J=8.1$  Hz), 7.78–7.84 (2H, t,  $H_{\text{aromat}}$ ), 7.19–7.49 (7H, m,  $H_{\text{aromat}}$ ), 6.81 (2H, dd,  $H_{\text{aromat}}$ ,  $J=47.7$ ,  $J=7.2$  Hz), 5.88 (1H, s, CHNH), 2.23 (3H, s,  $\text{CH}_3$ );  $^{13}\text{C}$  NMR (75 MHz, DMSO- $d_6$ ): 167.9, 164.8, 153.2, 146.7, 132.4, 130.6, 129.9, 129.3, 129.1, 129.0, 126.9, 125.8, 123.8, 122.9, 121.9, 119.8, 118.8, 94.4, 52.6, 12.5.

#### 1-[(4-Fluoro-phenyl)-(5-methyl-isoxazol-3-ylamino)-methyl]-naphthalen-2-ol (4i)

$^1\text{H}$  NMR (300 MHz, DMSO- $d_6$ ): 10.11 (1H, s, OH), 7.98 (1H, d, NH,  $J=8.1$  Hz), 7.76–7.83 (2H, m,  $H_{\text{aromat}}$ ), 7.36–7.41 (1H, t,  $H_{\text{aromat}}$ ), 7.25–7.33 (4H, m,  $H_{\text{aromat}}$ ), 7.06–7.012 (2H, t,  $H_{\text{aromat}}$ ), 6.77 (2H, dd,  $H_{\text{aromat}}$ ,  $J=7.5$  Hz,  $J=39.6$  Hz), 5.87 (1H, s, CHNH), 2.23 (3H, s,  $\text{CH}_3$ );  $^{13}\text{C}$  NMR (75 MHz, DMSO- $d_6$ ): 167.8, 164.9, 162.7, 159.5, 153.1, 139.7, 132.5, 129.7, 129.0, 128.5, 128.4, 126.7, 124.0, 122.8, 120.1, 118.8, 115.1, 114.9, 94.4, 52.5, 12.5.

#### 1-[(5-Methyl-isoxazol-3-ylamino)-(4-nitro-phenyl)-methyl]-naphthalen-2-ol (4j)

$^1\text{H}$  NMR (300 MHz, DMSO- $d_6$ ): 10.25 (1H, s, OH), 8.17 (2H, d,  $H_{\text{aromat}}$ ,  $J=8.7$  Hz), 7.95 (1H, d, NH,  $J=7.8$  Hz), 7.80–7.85 (2H, m,  $H_{\text{aromat}}$ ), 7.54 (2H, d,  $H_{\text{aromat}}$ ,  $J=8.7$  Hz), 7.38–7.43 (1H, t,  $H_{\text{aromat}}$ ), 7.26–7.30 (2H, m,  $H_{\text{aromat}}$ ), 6.90 (2H, dd,  $H_{\text{aromat}}$ ,  $J=6.6$  Hz,  $J=50.1$  Hz), 5.89 (1H, s, CHNH), 2.25 (3H, s,  $\text{CH}_3$ );  $^{13}\text{C}$  NMR (75 MHz, DMSO- $d_6$ ): 169.8, 168.0, 164.8, 153.3, 152.2, 146.3, 132.4, 130.2, 130.0, 129.1, 129.0, 128.9, 127.8, 127.7, 127.0, 124.4, 123.8, 123.6, 123.0, 119.4, 118.8, 118.4, 96.3, 94.4, 52.9, 12.5.

**9,9-Dimethyl-12-(phenyl)-8,9,10,12-tetrahydrobenzo[a]xanthen-11-one (6a)**

$^1\text{H}$  NMR (400 MHz,  $\text{CDCl}_3$ ): 7.00–8.07 (m, 10H, Ar–H), 5.59 (s, 1H, CH), 2.62 (s, 2H,  $\text{CH}_2$ ), 2.58 (d,  $J = 16.0$  Hz, 1H,  $\text{CH}_2$ ), 2.35 (d,  $J = 16.0$  Hz, 1H,  $\text{CH}_2$ ), 2.14 (s, 3H,  $\text{CH}_3$ ), 1.08 (s, 3H,  $\text{CH}_3$ ), 0.89 (s, 3H,  $\text{CH}_3$ ).

**9,9-Dimethyl-12-(4-methyl phenyl)-8,9,10,12-tetrahydrobenzo[a]xanthen-11-one (6b)**

$^1\text{H}$  NMR (400 MHz,  $\text{CDCl}_3$ ): 7.00–8.07 (m, 10H, Ar–H), 5.71 (s, 1H, CH), 2.62 (s, 2H,  $\text{CH}_2$ ), 2.58 (d,  $J = 16.0$  Hz, 1H,  $\text{CH}_2$ ), 2.35 (d,  $J = 16.0$  Hz, 1H,  $\text{CH}_2$ ), 2.14 (s, 3H,  $\text{CH}_3$ ), 1.08 (s, 3H,  $\text{CH}_3$ ), 0.89 (s, 3H,  $\text{CH}_3$ ).

**9,9-Dimethyl-12-(4-methoxy-phenyl)-8,9,10,12-tetrahydrobenzo[a]xanthen-11-one (6c)**

$^1\text{H}$  NMR (400 MHz,  $\text{CDCl}_3$ ): 6.72–8.07 (m, 10H, Ar–H), 5.69 (s, 1H, CH), 3.72 (s, 3H,  $\text{OCH}_3$ ), 2.59 (s, 2H,  $\text{CH}_2$ ), 2.36 (d,  $J = 16.0$  Hz, 1H,  $\text{CH}_2$ ), 2.30 (d,  $J = 16.0$  Hz, 1H,  $\text{CH}_2$ ), 2.25 (s, 3H,  $\text{CH}_3$ ), 1.15 (s, 3H,  $\text{CH}_3$ ), 1.00 (s, 3H,  $\text{CH}_3$ ).

**Supplementary Information** The online version contains supplementary material available at <https://doi.org/10.1007/s11164-021-04558-9>.

**Acknowledgements** We gratefully acknowledge the financial support from the Research Council of the University of Sistan and Baluchestan

**References**

1. R.S. Varma, A. C. S. Sustainable. Chem. Eng. **4**, 5866 (2016)
2. M. Kaushik, A. Moores, Opin Green Sustainable Chem. **7**, 39 (2017)
3. L.L. Chng, N. Erathodiyil, J.Y. Ying, Acc. Chem. Res. **46**, 1825 (2013)
4. R.G. Chaudhuri, S. Paria, Chem Rev. **112**, 2373 (2012)
5. S.J. Oldenberg, R.D. Averitt, S.L. Westcott, N.J. Halas, Chem. Phys. Lett. **288**, 243 (1998)
6. M.B. Gawande, R. Luque, R. Zboril, Chem. Cat. Chem. **6**, 3312 (2014)
7. R.B.N. Baig, M.N. Nadagouda, R.S. Varma, Coord. Chem. Rev. **287**, 137 (2015)
8. D. Wang, D. Astruc, Chem. Rev. **114**, 6949 (2014)
9. T. Cheng, D. Zhang, H. Li, G. Liu, Green Chem. **16**, 3401 (2014)
10. R.B.N. Baig, S. Verma, R.S. Varma, M.N. Nadagouda, A.C.S. Sus, Chem. Eng. **4**, 1661 (2016)
11. V. Polshettiwar, R. Luque, A. Fihri, H.B. Zhu, M. Bokhara, J.M. Bassett, Chem. Rev. **111**, 3036 (2011)
12. B.L. Li, M. Zhang, H.C. Hu, X. Du, Z.H. Zhang, New J. Chem. **38**, 2435 (2014)
13. X.X. Zhang, J.S. Bradshaw, R.M. Izatt, Chem. Rev. **97**, 3313 (2007)
14. W. Wang, F. Ma, X. Shen, C. Zhang, Tetrahedron Asymmetry **18**, 832 (2007)
15. S. Maeng, C.A. Zarate, J. Du, R.J. Schloesser, J. McCammon, G. Chen, H.K. Manji, Biol. Psychiatry. **63**, 349 (2008)
16. N. Mulakayala, P.V.N.S. Murthy, D. Rambabu, M. Aeluri, R. Adepu, G.R. Krishna, C.M. Reddy, K.R.S. Prasad, M. Chaitanya, C.S. Kumar, M.V.B. Rao, M. Pal, Bioorg Med. Chem. Lett. **22**, 2186 (2012)
17. G.W. Rewcastle, G.J. Atwell, L.Z. Huang, B.C. Baguley, W.A. Denny, J. Med. Chem. **34**, 217 (1991)

18. H. Faroughi niya, N. Hazeri, M. Rezaie kahkhaie, M.T. Maghsoodlou, *Res. Chem. Intermed.* **46**, 1685 (2020)
19. H. Faroughi Niya, N. Hazeri, M.T. Maghsoodlou, *Appl. Organometal. Chem.* **34**, e5472 (2020)
20. M. Fatahpour, F. Noori Sadeh, N. Hazeri, M.T. Maghsoodlou, M.S. Hadavi, S. Mahnaei, *J. Saudi Chem. Soc.* **21**, 8998 (2017)
21. R. Doostmohammadi, N. Hazeri, *Lett. Org. Chem.* **10**, 199 (2013)
22. N. Hazeri, M.T. Maghsoodlou, N. Mahmoudabadi, R. Doostmohammadi, S. Salahi, *Curr. Organo. catal.* **1**, 45 (2014)
23. M. Safarzaei, M.T. Maghsoodlou, E. Mollashahi, N. Hazeri, M. Lashkari, *Res. Chem. Intermed.* **44**, 7449 (2018)
24. Q. Zhang, H. Su, J. Luo, Y. Wei, *Green Chem.* **14**, 201 (2012)
25. F. Shirini, M. Abedini, R. Pourhasan, *Dyes Pigm.* **99**, 250 (2013)
26. X.J. Sun, J.F. Zhou, P.S. Zhao, *J. Heterocycl. Chem.* **48**, 1542 (2011)
27. G.C. Nandi, S. Samai, R. Kumar, M.S. Singh, *Tetrahedron* **65**, 7129 (2009)
28. A. Khazaiea, M.A. Zolfigol, A.R. Moosavi-Zare, A. Zare, M. Khojasteh, Z. Asgari, V. Khakyzadeh, A. Khalafi-Nezhadd, *Catal. Commun.* **20**, 54 (2012)
29. R.Z. Wang, L.F. Zhang, Z. Shui, *Synth. Commun.* **39**, 2101 (2009)
30. B. Das, K. Laxminarayana, M. Krishnaiah, Y. Srinivas, *Synlett* **20**, 3107–3112 (2007)
31. M. Fatahpour, N. Hazeri, M.T. Maghsoodlou, M. Lashkari, *Iran. J. Sci. Technol. Trans. A Sci.* **42**, 533 (2018)
32. R. Mohammadi, E. Eidi, M. Ghavami, M.Z. Kassaei, *J Mol Catal. A Chem.* **393**, 309 (2014)
33. Q. Zhang, H. Su, J. Luo, Y. Wei, *J. Green Chem.* **14**, 201 (2012)
34. H.T. Nguyen, N.P. Le, D.K. Chau, P.H. Tran, *RSC Adv.* **8**, 35681 (2018)
35. L. Kheirkhah, M. Mamaghani, A. Yahyazadeh, N. Mahmoodi, *Appl. Organometal. chem.* **32**, e4072 (2018)
36. Z. Kheilkordi, G. MohammadiZiarani, N. Lashgari, A. Badiei, *Polyhedron* **166**, 203 (2019)
37. A. Maleki, M. Aghaei, N. Ghamari, *Appl. Organometal. Chem.* **30**, 939 (2016)
38. M. RezaieKahkhaie, N. Hazeri, M.T. Maghsoodlou, A. Yazdani-Elah-Abadi, *Iran. J. Sci. Technol. Trans. A Sci.* **5**, 422 (2020)

**Publisher's Note** Springer Nature remains neutral with regard to jurisdictional claims in published maps and institutional affiliations.

## Authors and Affiliations

Mahboobeh Rezaie Kahkhaie<sup>1</sup> · Nourallah Hazeri<sup>1</sup> ·  
Malek Taher Maghsoodlou<sup>1</sup> · Afshin Yazdani-Elah-Abadi<sup>2</sup>

<sup>1</sup> Department of Chemistry, Faculty of Science, University of Sistan and Baluchestan, P.O. Box 98135-674, Zahedan, Iran

<sup>2</sup> Department of Biology, Science and Art University, Yazd, Iran